# Supporting Information

Yi et al. 10.1073/pnas.0906553106

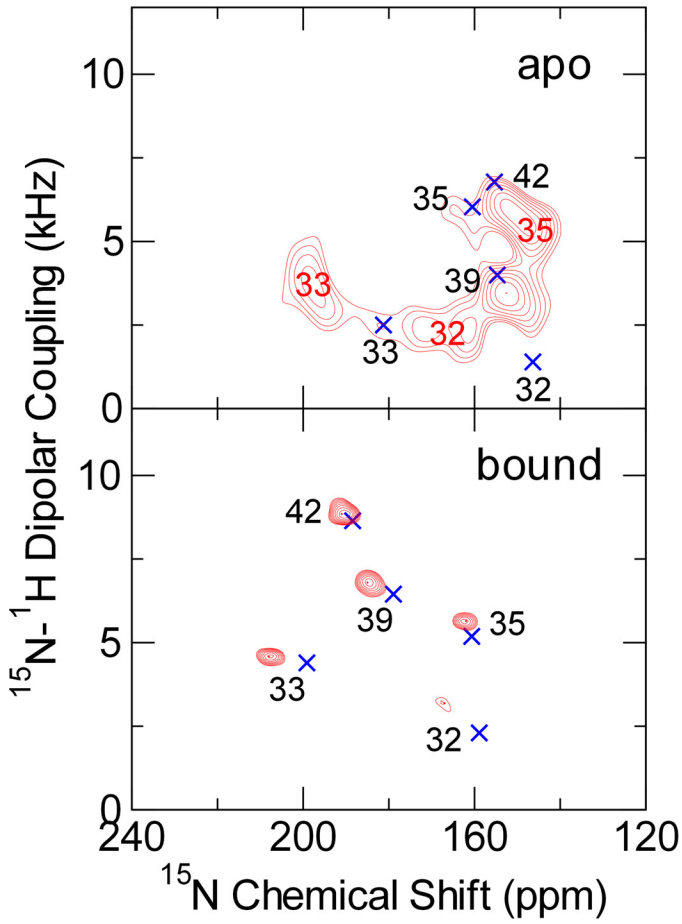


**Fig. S1.** PISEMA spectra of 5 Ile residues (at positions 32, 33, 35, 39, and 42) in apo and amantadine-bound M2 TMD measured by solid-state NMR (red) and calculated from MD trajectories (blue, averaged over all 4 helices and over 2 trajectories). The measured PISEMA spectra are taken from Li C, Qin H, Gao FP, and Cross TA [(2007) Solid-state NMR characterization of conformational plasticity within the transmembrane domain of the influenza A M2 proton channel. *Biochim Biophys Acta* 1768:3162–3170]. The individual results for each of 5 Leu residues (at positions 26, 36, 38, 40, and 43) collected from the 4 helices over 2 MD trajectories, before averaging, are shown in Fig. 3.

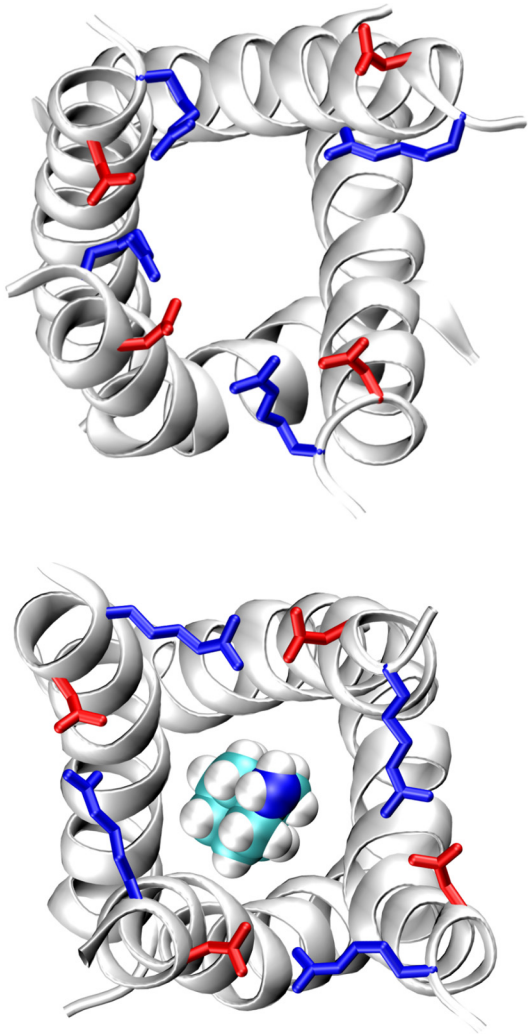

**Fig. S2.** Interhelical and intrahelical salt bridges between Asp-44 and Arg-45. The apo form (*Upper*) is dominated by intrahelical salt bridges, whereas the amantadine-bound form (*Lower*) is dominated by interhelical salt bridges.

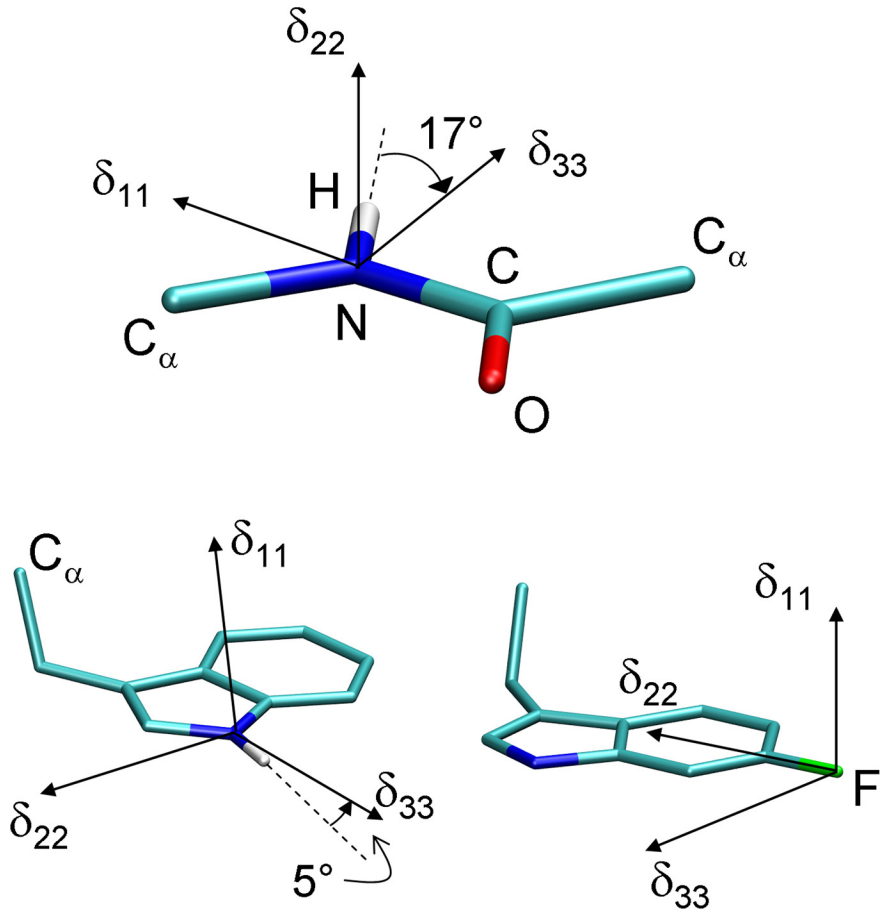


**Fig. S3.** Directions of the principal axes of $^{15}N$ and $^{19}F$ chemical-shift tensors in the molecular frames of peptide backbone and Trp side chain. For backbone $^{15}N$, $\hat{\delta}_{22}$ is perpendicular to the peptide plane, and $\hat{\delta}_{33}$ is obtained by rotating the N-H vector around the $\hat{\delta}_{22}$ axis clockwise (toward the carbonyl carbon) for 17° (1). For Trp sidechain $^{15}N$, $\hat{\delta}_{22}$ is in the indole ring and perpendicular to the N-H vector, and $\hat{\delta}_{33}$ is obtained by rotating the N-H vector around the $\hat{\delta}_{22}$ axis counterclockwise for 5° (2). For $^{19}F$ at the 6F-Trp position, $\hat{\delta}_{22}$ is along the F-C vector, and $\hat{\delta}_{33}$ is in the indole ring (and perpendicular to $\hat{\delta}_{22}$) (3).


1. Wang J, et al. (2000) Imaging membrane protein helical wheels. *J Magn Reson* 144:162–167.
2. Ramamoorthy A, Wu CH, Opella SJ (1997) Magnitudes and orientations of the principal elements of the $^{1}H$ chemical shift, $^{1}H$–$^{1}N$ dipolar coupling, and $^{15}N$ chemical shift interaction tensors in $^{15}N^{\epsilon 1}$-tryptophan and $^{15}N^{\pi}$-histidine side chains determined by three-dimensional solid-state NMR spectroscopy of polycrystalline samples. *J Am Chem Soc* 119:10479–10486.
3. Witter R, et al. (2008) Solid-state $^{19}F$ NMR spectroscopy reveals that Trp41 participates in the gating mechanism of the M2 proton channel of influenza A virus. *J Am Chem Soc* 130:918–924.

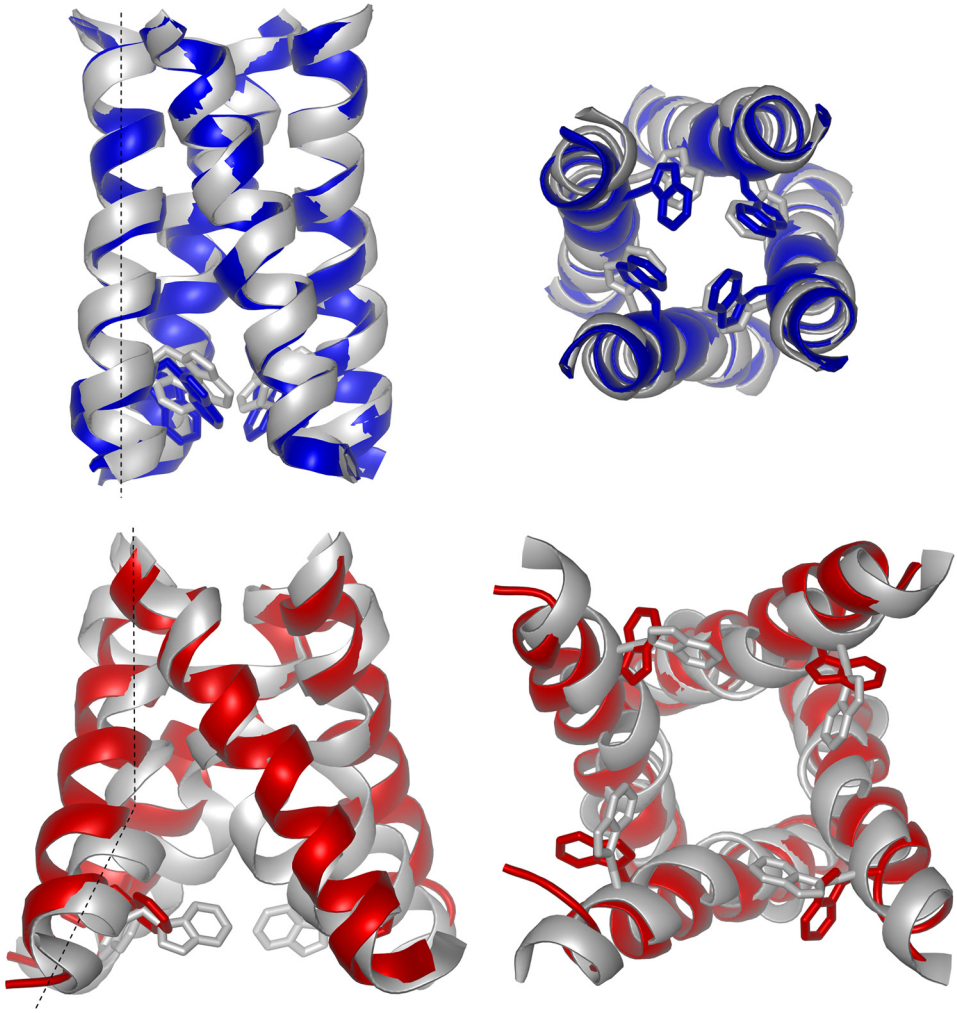

**Fig. S4.** Representative structures, shown in gray, for the unprotonated (*Upper*) and protonated (*Lower*) states. For each structure, *Left* and *Right* show views within the membrane bilayer and from the virus interior side, respectively. Straight and bent lines in the *Upper* and *Lower Left* indicate the small and large helix-kink angles, respectively, of the unprotonated and protonated models. Superimposed to these models are structures determined by solution NMR [Protein Data Bank (PDB) ID code 2RLF] (1) and X-ray crystallography (PDB ID code 3C9J) (2), shown in blue and red, respectively. The superposition suggests that the representative structure for the unprotonated state is similar to the NMR structure, determined at a relatively high pH of 7.5, whereas the representative structure for the protonated state is similar to the X-ray structure determined at a low pH of 5.3 (note that both structures were determined in the presence of a drug molecule). Superposition was over the N-terminal half (residues Leu-26–Gly-34) only. For clarity, only the portion from Leu-26 to Leu-46 is shown. Trp-41 side chains are shown as sticks.


1. Schnell JR, Chou JJ (2008) Structure and mechanism of the M2 proton channel of influenza A virus. *Nature* 451:591–595.
2. Stouffer AL, et al. (2008) Structural basis for the function and inhibition of an influenza virus proton channel. *Nature* 451:596–599.

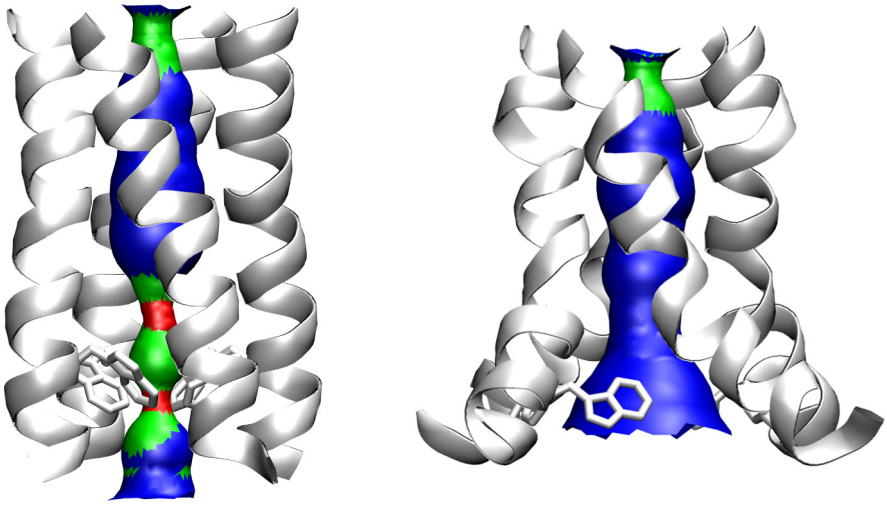

**Fig. S5.** Channel pores in the models of the unprotonated (*Left*) and protonated (*Right*) states. Pore radii are calculated by the HOLE program [Smart OS, Neduvelil JG, Wang X, Wallace BA, Sansom MS (1996) HOLE: A program for the analysis of the pore dimensions of ion channel structural models. *J Mol Graphics* 14:354–360:376] and color-coded as follows: red, $<$ 1.15 Å; green, between 1.15 and 2.30 Å; and blue, $>$ 2.30 Å. Trp-41 side chains are shown as sticks.

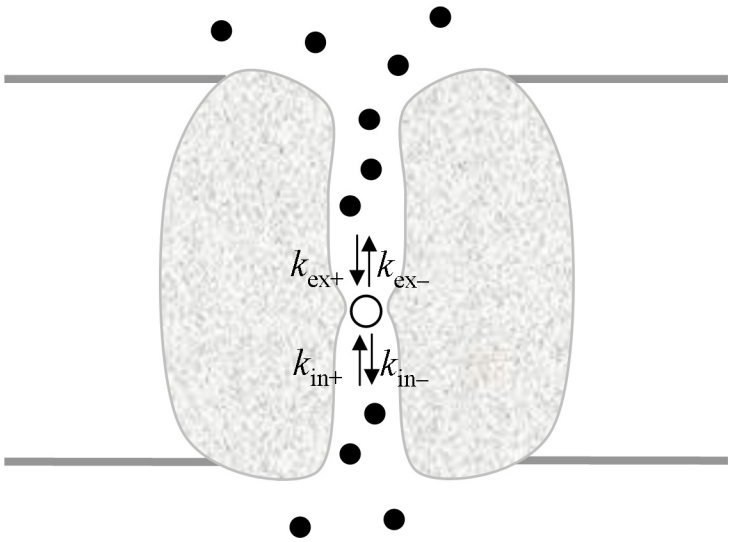


**Fig. S6.** Kinetic model for proton conductance. The open circle represents the binding site presented by His-37; smaller black circles represent protons.

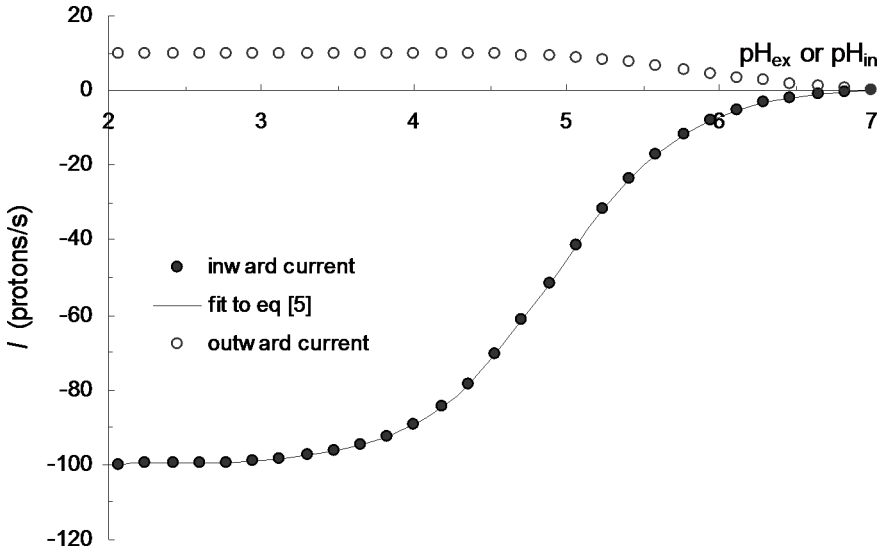


**Fig. S7.** Proton flux predicted by the kinetic model. The abscissa is $pH_{ex}$ for inward current and $pH_{in}$ for outward current.

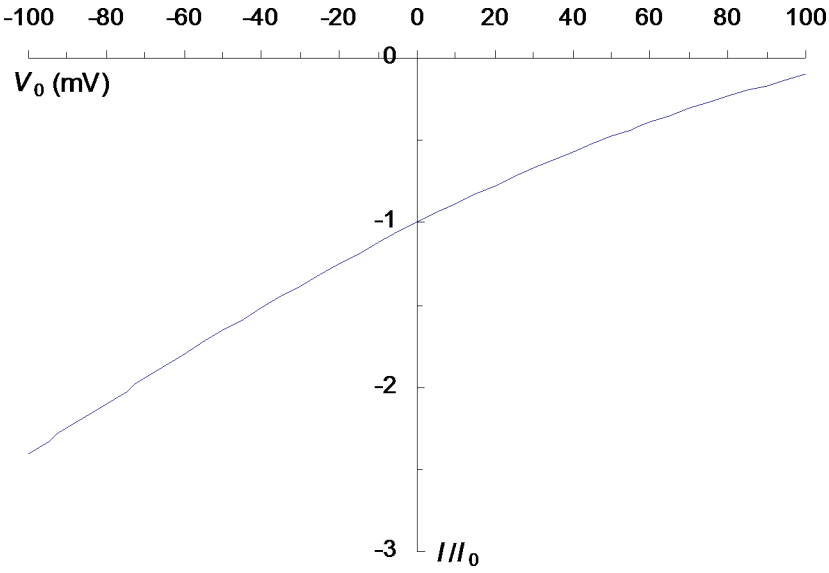


**Fig. S8.** Voltage-proton flux relation. Following Chizhmakov et al. [(2003) Differences in conductance of M2 proton channels of two influenza viruses at low and high pH. *J Physiol (London)* 546:427–438], a negative sign is assigned to $I/I^0$ to indicate inward flux.

## Other Supporting Information Files

*SI Appendix* (PDF)